



Seismic Retrofit Strategies for Historic Masonry Bridges: A Case Study Including Soil–Structure Interaction

Pınar USTA EVCI^{1,}, Cemile ÜNVEREN¹, Ali Ekber SEVER¹ and Elifnur ŞAKALAK¹*

¹ Isparta University of Applied Sciences, Faculty of Technology Department of Civil Engineering, 32260 Isparta, Türkiye

SUMMARY: *The aim of this analysis is to examine the seismic behavior of the historic Cirimbolu Bridge via two different models developed with the computer program SAP2000. The first model simulated the soil under the bridge, and the seismic behavior of the historic Cirimbolu Bridge with regard to the interaction of soil and the effects of soil-structure interaction behavior was examined. The second model simulated the historic Cirimbolu Bridge as being fixed to the ground. The analysis was performed using acceleration data relevant to the Pazarcık and Elbistan earthquakes, and these earthquakes happened in Turkey on February 6, 2023. The results of both models indicated similar periods and mode shapes; however, SSI contained increased values of frequency. The models' displacement and stress results were calculated via linear analysis of both models performed via the time domain method. The largest displacement is calculated at the top of the bridge via both models. Significant decreases in displacement and stress values of the models are calculated when simulating the soil as fixed. Moreover, the fixed soil model results are supplemented with different strengthening methods such as steel tendons, CFRP, and FRCM. The analysis results show that steel tendon reinforcement is successful.*

KEYWORDS: *masonry bridge, strengthening, seismic analysis, soil structure interaction, Türkiye*

1 Introduction

Masonry arch bridges form the essential element of transport infrastructure in many parts of the world and also extremely valuable cultural and architectural heritage. They are prone to irreparable partial or total damage by some unforeseeable events of nature, such as earthquakes. Natural disasters, such as earthquakes and floods, may affect these structures and cause serious damage or even their total destruction. It is thus essential for the survival of masonry arch bridges to develop finite element models and analyze their static and dynamic behaviors by using computer programs.

Masonry arch bridges are significant both in worldwide transportation systems and as a valued cultural and architectural heritage. These types of bridges are prone to partial or complete destruction due to some unpredictable actions such as earthquakes. These structures can be seriously damaged or totally destroyed by natural hazards, including earthquakes and flood. Therefore, there is an urgent need to develop finite element models and analyze static

and dynamic behaviours of masonry arch bridges in some computer programs with a view to ensuring their survival.

There are numerous studies in the literature which search for the seismic performance of masonry structure and especially bridges; however, the structure-soil interaction effect was seen to be largely avoided. For example, Kader et al. [1] investigated the seismic behaviour of the masonry arch bridge with various damping ratios. The seismic performance of the bridge was investigated with a computer simulation carried out in the SAP2000 computer program. The stress and displacement values acquired by the time history analysis in a linear manner were calculated on the bridge. It was seen that the displacement and stress values in the bridge decreased with the increase of the damping ratio.

In a recent research, Shabani et al. [2] performed a seismic analysis on a historic masonry arch bridge. They used the finite element method in DIANA computer programming. During time history analysis, different acceleration records were used, and results showed that the bridge satisfied the required SPS level of security. The researchers suggested that it is necessary to improve and strengthen the bridge arch, and spandrel walls between the arches. Sakcalı et al. [3] performed research on an existing masonry arch bridge, named Irgandı Bridge. It is in Bursa. A finite element method model was created, and results were obtained using an ANSYS programming. Modal and time history analysis, using different acceleration records, were used. From the modal analysis, the researchers obtained the results, which included the periods and mode shapes of the bridge. Moreover, results of time history analysis showed that there were the highest values of displacements at the top of the bridge, and in the abutment region, there were the highest values of principal stress.

In their study, Yılmaz et al. [4] considered the seismic behaviour of the Murat Bey Bridge, which was built as a masonry arch bridge. In this regard, modelling the mentioned bridge was done within the scope of the study using the computer program called SAP2000. During the course of this study, the authors found that the maximum stress values that developed within the bridge were determined, wherein the maximum compressive stresses were found at the grounds, while the maximum tensile stresses were found within the spandrel walls at the edges. Moreover, within the scope of the study carried out by Sözen and Çavuş [5], an investigation into the seismic behaviour related to the structural analysis of a historic masonry arch bridge was performed, wherein the authors were enabled, within their modelling, using the computer program known as ANSYS, to create the original and altered versions of the mentioned structure. In this regard, the rigidity related to the structure was seen to have enhanced due to alterations.

The aforementioned studies examined the seismic behavior of the bridges assuming the fixed nature of the supports and ignoring the concept of SSI. The interaction of the structures with the surrounding soil media has been found effective in producing a change in the dynamic characteristics of the structures due to time-dependent loads, as proposed by Wolf [6] and Kramer [7]. A significant amount of literature can be found focusing on the seismic behavior of structures incorporating the concept of SSI.

This is an important issue since modeling the bridge and the underlying soil together significantly affects the dynamic behaviour of bridges [8]. There are many studies in the literature regarding seismic behaviour of masonry arch bridges taking into account structure-soil interaction. Zani et al. [9] conducted a study regarding the dynamic behaviour of a historic masonry arch bridge in Italy. To do this, they generated finite element models using the ABAQUS computer program by assuming fixed supports and taking into account the interaction between the structure and the soil. They performed modal analysis and time history analysis on the mentioned models. The obtained modal analysis results indicated that

the model taking into account the structure-soil interaction provided higher period values. The displacements obtained with the time history analyses were lower for the model assuming fixed sup-ports.

Güllü and Jaf [10] did a research and performed an experiment with the aim of investigating and discovering the effects of the interaction of soil and structures on the seismic behavior of a masonry arch bridge. The researcher developed two separate models via a computer program and performed both modal and time history analysis with the aim of investigating the effects of the interaction of soil and structures. By carrying out the modal analysis, the researcher found effects of interaction of soil with structures; specifically, the results indicated smaller period values when fixed supports are assumed. During the time-history analysis, the researcher found effects of interaction of soil with structures; specifically, lower displacement values when fixed supports are assumed. The researcher concluded the review of the case with emphasis laid upon the importance of detailed modeling of structure-soil interaction with the aim of evaluating seismic behavior of masonry arch bridges accurately.

A study was carried out by Özmen and Sayın [11], the main objective being the exploration of the effects that structure-soil interaction has on the seismic behaviour of a single-span historic masonry arch bridge. In achieving this objective, the researchers developed models via the DIANA computer program, based on structure-soil interaction. Various support models were considered. It was found that the mode structure-soil interaction increases the values related to the period, displacements, and principal stresses. A key observation was the fact that the structure-soil interaction has considerable influence on seismic behaviour.

Awlla et al. [12] in their research paper, investigated the seismic behavior of a historic bridge by considering comparison with the dynamic response of the bridge model while using fixed supports, as well as structure-soil interaction. The authors used three soil profile conditions, namely, stiff, medium, as well as soft soil profile conditions, while carrying out the structure-soil interaction. The seismic analysis indicated significant correlations between fixed support model as well as stiff soil profile condition. However, significant discrepancies were observed while using medium soil profile conditions as well as soft soil profile conditions.

Investigation of seismic behavior of the historic masonry arch bridge was performed within the context of the research conducted by Rovithis and Pitilakis [13]. They used a computer program to develop finite element models of the bridge with various support types. The results of the relevant analysis indicated, among other instances, that the increased evaluation of the value of the natural period of the concerned bridge due to the presence of soil-structure interaction effects was significant.

The existing structures, which have been determined as inadequate in terms of seismic analysis, should be strengthened. There is significant research in this area in relation to the issue of strengthening. These studies were discussed briefly as follows.

It is evident that historical arch bridges play a significant role in the continuity of cultural heritage. In order to prevent the aforementioned structures from being damaged as a result of disasters such as floods and earthquakes, it is necessary to model and analyse them in computer programs. In order for the results of the analysis to be as accurate as possible, it is necessary to consider the interaction between the structure and the soil. For these reasons, the seismic performance of a historical masonry arch bridge in Turkey was investigated by taking structure-soil effects into consideration. Various strengthening suggestions were presented to enable the structure to withstand seismic loads.

The study investigated the seismic performance of the historic Cirimbolu Bridge located in Uluborlu district of Isparta, Türkiye. Two different finite element models were created in the SAP2000 computer program for this purpose. Within the scope of the study, two different bridge models were created with fixed supports and soil-structure interaction. Modal analysis and time history analyses were performed on these models. Then, different strengthening methods were numerically applied to the fixed support model and the results were evaluated.

2 Seismicity of Isparta

Isparta is situated in the Mediterranean region and falls within the first-degree seismic zone [14]. The Isparta-Dinar-Çivril-Uşak fault line runs through the province. Yenişarbademli and Sütçüler districts have a second degree earthquake risk, while a small area to the east of Sütçüler carries a third-degree earthquake risk. About 93% of the population lives in the first-degree earthquake zone [15]. Figure 1 shows the tectonic map of the region where Isparta is located.

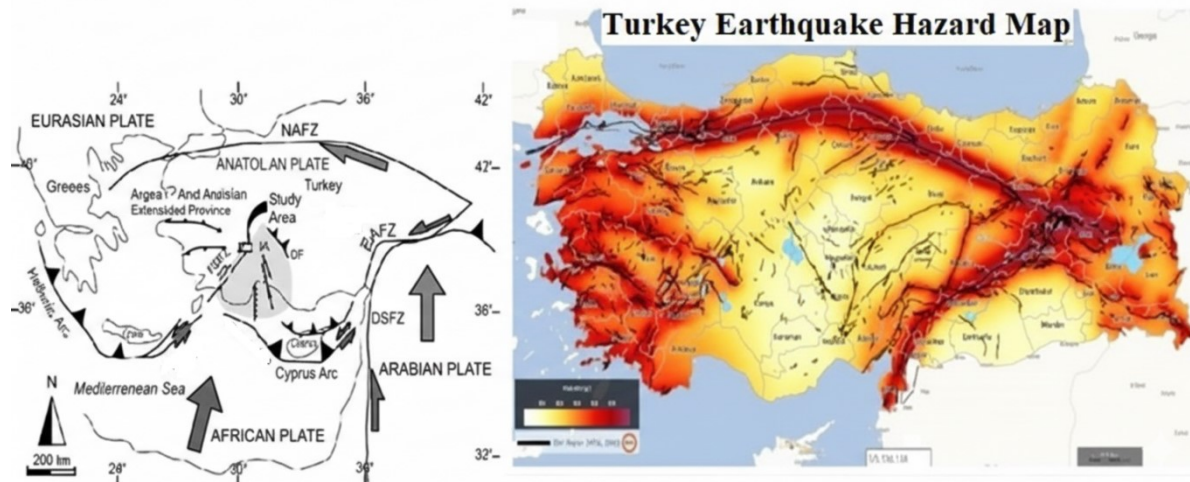
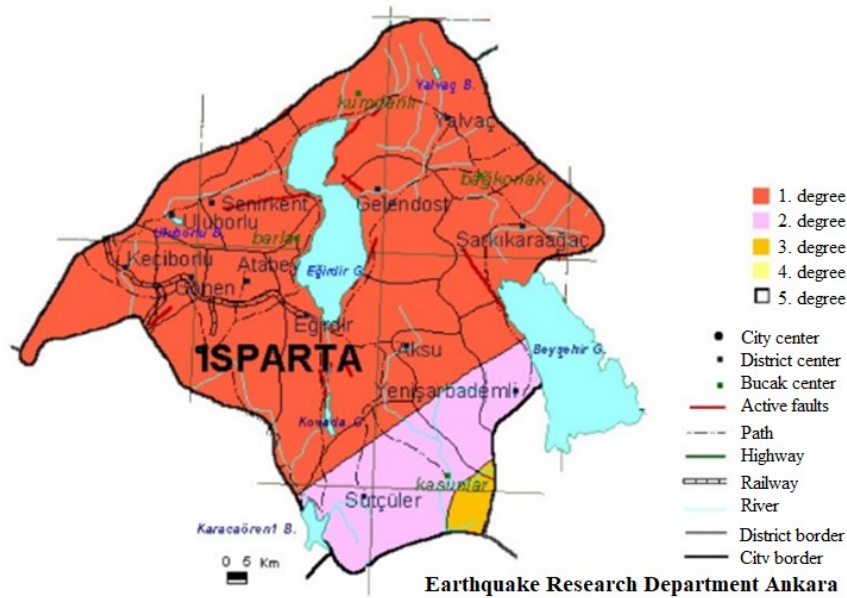


Figure 1: Tectonic map showing the region where Isparta is located.

Isparta and its surrounding areas have a history of experiencing earthquakes, and it is possible that new earthquakes may occur in the region. Table 1 [15] lists some of these earthquakes.

Table 1: Some earthquakes that occurred in Isparta province and its surroundings [15]

Date	Area	Fault	Ms1	Io2
2002	Sultandağı	Sultandağı	6.5	VIII
1995	Dinar	Dinar	6.1	IX
1971	Burdur	Burdur	6.2	IX
1933	Dinar	Balkan	5.8	VIII
1925	Dinar	Balkan	6	VIII-IX
1914	Burdur	Burdur	7.1	IX
1889	Isparta	?	?	?
1875	Dinar	Balkan	?	IX-X

Table 1 shows that earthquakes in the region have a minimum magnitude of 5.8 and are categorized as destructive. This indicates a high probability of earthquakes causing damage to structures.

3 Material and method

3.1 Historical Cirimbolu Bridge

The Cirimbolu Bridge and Aqueduct are situated in the initial settlement regions of Uluborlu. The bridge is located at latitude 38.08453 and longitude 30.47519. The bridge was constructed between 1869 and 1872 with the intention of transporting water from Kaviil Spring to Uluborlu Castle on Kapı Mountain. The arch, which can also serve as a bridge, is constructed on top of two stacked round arches. A survey project was conducted to measure the historic bridge and aqueduct on-site. The Cirimbolu Bridge has a width of 3 m, a height of 21 m, and a length of 45 m, as measured. There are two 6.8 m long circular wooden beams on the upper arch of the bridge and four 4.5 m long circular wooden tensioners on the lower arch. The diameter of these beams is 15 cm. Figure 2 illustrates the location of the bridge and the bridge itself.



Figure 2: Historical Cirimbolu bridge and its location

The historical bridge and aqueduct have not undergone any restoration work and remain in their current state. They are not suitable for vehicle traffic.

A comprehensive measurement process is implemented to accurately determine and evaluate the internal part of bridges. This process involves the precise measurement of the interior of the structure and the use of various advanced techniques to gain a detailed understanding of the structure. It comprises a number of multi-process procedures, including laser scanning, ground-penetrating radar (GPR), ultrasonic testing, infrared thermography, drilling and core sampling, as well as ground mechanics. It also necessitates the undertaking of special studies on the subject. In this study, the initial stage of the process, namely visual examination, was carried out in accordance with the stated purpose of the article.

A survey was conducted to assess the current condition of the building and to update its plans and sections. Based on the survey, a 3D solid model of the building was created using the AutoCAD program. Figure 3 shows the appearance of the upstream and downstream facades of the bridge and aqueduct, depending on the measurements taken.

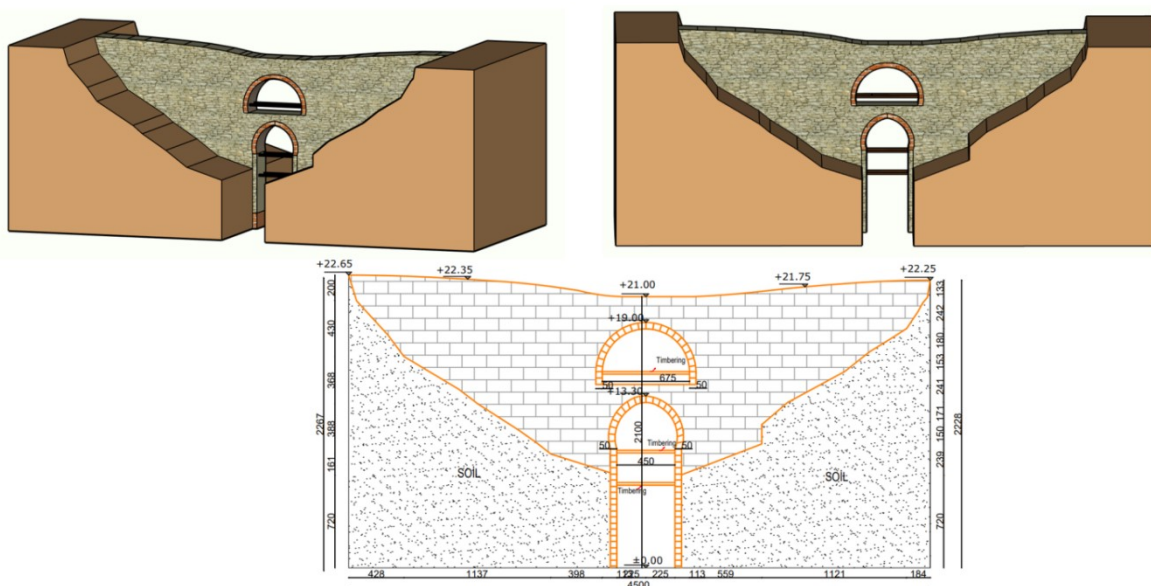


Figure 3: Cirimbolu Bridge perspectives.

3.2 Determination of material properties for historical bridge and aqueducts

The bridge and aqueduct in Uluborlu, Isparta were built using rubble stone and mortar. The study investigated the chemical, mechanical, and physical properties of the materials used in the structure's construction. The material properties of historical structures can be determined through laboratory experiments using samples and on-site measurements. However, conducting such experiments can be risky as they may disrupt the structure's integrity and cause damage. In this study, fallen stones from the bridge were used to determine the material properties of the bridge and aqueduct. The experimental studies utilized both non-destructive and destructive methods.

The stones or bricks that constitute masonry buildings are held together by mortar to form a composite element. This composite element is treated as a single entity in practical analyses of masonry buildings.

The static modulus of elasticity of masonry stones, as outlined in various standards, can be empirically calculated. The first equation provides a method for determining the modulus of elasticity based on the compressive strength [16].

The equation is as follows:

$$E_{mas} = 750 * f_{c_{mas}} \quad (1)$$

Where $f_{c_{mas}}$ (MPa) represents the characteristic compressive strength of the stone, and E_{mas} (MPa) represents the modulus of elasticity of the stone.

In this study, it is observed that the average compression strengths of the samples of stone is calculated as 4.353 (MPa). In the absence of experimental data, it was hypothesised that the Poisson's ratio would be equivalent to 0.2.

The unit volume weight of the stone sample of the historical bridge was found to be 23.6 kN/m³ according to the TS EN 12 390-7 standard as a result of the studies and mathematical calculations. The modulus of elasticity was calculated as 3250 MPa using equation (1).

Wood, a material that is readily processed and transported, has been employed from antiquity to the present due to its resilience to bending, tensile, and compressive stresses, as well as its lightweight nature [17]. The anisotropic nature of wood material makes it challenging to examine its mechanical properties. The mechanical properties of the wooden tension elements utilised in the arch sections of the bridge were derived from studies conducted in the literature [18]. The elasticity modulus of the wooden tensioner was found to be 3000 kg/cm² in the perpendicular direction to the fibers and 100000 kg/cm² in the parallel direction. The Poisson ratio and density of the wooden tensioner were assumed to be 0.3 and 0.5 g/cm³, respectively.

3.3 Calculation of safety stresses of the bridge

According to the 2018 Turkey Building Earthquake Regulation [16], the recommended pressure safety stress for stone masonry walls is 0.3 MPa. It is worth noting that the safety stress has been increased threefold. To calculate the safety stress (f_{em}) for masonry walls, use the following formula.

$$f_{em} = 3 \times 0.3 = 0.9 \text{ Mpa}$$

Tensile safety stress is accepted as 15% of the pressure safety stress value. Tensile safety stress (f_{emc}) for masonry walls is calculated as follows [17, 19].

$$f_{em\check{c}} = 0.15 \times 0.9 = 0.135 \text{ Mpa}$$

The shear stresses obtained from the earthquake calculation are compared with the shear limit stress calculated according to Equation 1.

$$\tau_m = \mu\sigma + \tau_o \quad (1)$$

In equation (1), τ_m refers to the shear limit stress, μ is the friction coefficient, σ is the wall vertical stress, and τ_o is the wall cracking safety stress. The cracking stress (τ_o) for the stone wall was calculated. According to Equation 1, τ_m was calculated as 0.53 MPa.

Accepted safety stresses for stone are given in Table 2 [16].

Table 2: Safety stress values of the materials used [16]

Material	Pressure Safety Stress Value (MPa)	Tensile Safety Stress Value (MPa)	Shear Safety Stress Value (MPa)
Arches and Masonry Walls	0.9	0.135	0.53

4 Creation of the finite element model of Cirimbolu Bridge

The Cirimbolu Bridge, a historical arch bridge, was modelled using the SAP2000 computer program. Modal and time history analyses were conducted on the solid element model of the arch structure. Figure 4 displays the axes, stresses, and solid element definition. S11 represents the stress acting on face 1 in the direction of axis 1, S22 represents the stress acting on face 2 in the direction of axis 2, S33 represents the stress acting on face 3 in the direction of axis 3, S12 represents the shear stress acting on face 1 in the direction of axis 2, S13 represents the shear stress acting on face 1 in the direction of axis 3, and S23 represents the shear stress acting on face 2 in the direction of axis 3 according to SAP2000.

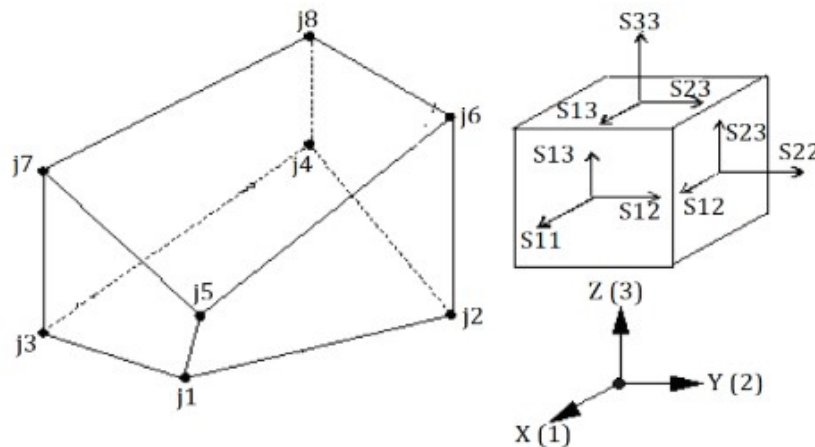


Figure 4: Solid element and stresses in the solid element

The SAP2000 computer program was used to create two different finite element models of the Cirimbolu bridge. One model, FS, anchors the bridge to the ground, while the other model, SSI, takes into account the structure-soil interaction. Figure 5 illustrates the FS model.

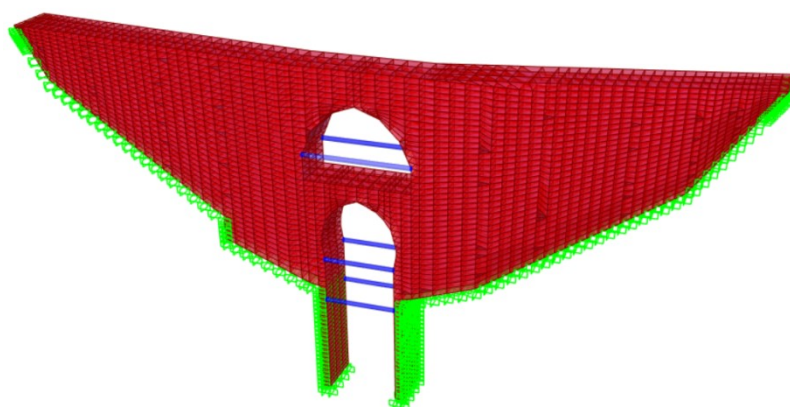


Figure 5: FS model.

The solid elements of SAP2000 were employed in the construction of the bridge models. In order to obtain accurate results from the finite element model, it is of the utmost importance to determine the number of mesh elements.

In the study, the following activities were performed, ensuring that the FE grid that was adopted converges toward actual responses. First, the type of grid density was considered, which improves the model's accuracy. For this purpose, the grid density was decided based on the complexity of the model adopted. Another activity was the choice of the type of elements. According to the nature of the structures that were examined, the relevant type of elements was adopted. To evaluate the accuracy of the adopted FE grid, the sensitivity analysis was performed. Various densities and sizes of elements, or meshes, were also tested. During this time, the results from the model were also examined. Also, analyses were done to ensure a conducive environment, which determined the most suitable kind of mesh. During this time, updates were made to improve the model. Various parameters, which updated the material, boundaries, and loadings, were made to fit better. This ensured an updated model, hence better output from the model. After all these processes, it was evident that the implemented FE mesh and model converged correctly to actual responses, thus improving the overall accuracy of the model.

There are usually three different approaches to numerical modelling of masonry structures, depending on the scale of the structural system and the required accuracy: simplified micro modelling, detailed micro modelling, and macro modelling [20]. Detailed micro modelling involves independent assessment of material properties of the masonry units and mortar. Simplified micro modelling is performed by extending the masonry units by half of the width of the mortar layer, while the mortar itself is neglected. The units are separated from each other by interface lines. In contrast, in macro modelling, masonry is considered as a single composite material without differentiating units and mortar. This approach drastically cuts down the time required for analysis of large structural systems and, therefore, is usually preferred for such applications. Macro modelling was used for this study, whereby the relationship between mortar and masonry units was neglected. The material was treated as a composite and homogenisation techniques were not employed [21]. In this study, macromodeling was chosen primarily because of its computational efficiency and the scale of the structure being analysed. Considering that masonry bridges are large and complex systems, a detailed micromodeling approach requiring explicit representation of individual units and mortar joints would significantly increase the computational cost and analysis time. This limitation has been widely recognised in previous studies of numerical modelling of historic masonry structures. In addition, macromodels provide global response estimates that are

accurate enough for large scale seismic analyses, which is consistent with the objectives of this study. While it is true that micromodeling can capture local effects such as mortar joint behaviour and anisotropic properties, several studies [22, 23] have shown that macromodeling is a reliable approach to evaluate the overall structural performance of masonry bridges under seismic loading, especially when the primary interest is in global displacements, mode shapes and stress distributions.

A convergence study was conducted with the objective of determining the optimal mesh density in the mathematical model of the historical bridge. A decision was made to use a mesh density where the results varied insignificantly. In the bridge's FS model 5643 solid and 8073 nodes elements were used.

A three-dimensional model of the structure was then created, and the material properties of the Cirimbolu bridge and aqueduct, obtained through experimentation, were defined in the model. A review of the literature was conducted in order to determine the material properties that should be used in the soil modelling. The stiff soil properties, analogous to those observed in the region where the historical bridge is situated, were adopted in accordance with the findings of Kramer [7], Bayraktar and Hökelekli [24]. Table 3 presents the material properties employed in the finite element models.

Table 3: Properties of the materials used [7, 24]

Material	Modulus of Elasticity (N/mm ²)	Poisson's Ratio	Density (kN/m ³)
Stone	3250	0,20	23.6
Hard soil	5570	0.3	26

4.1 SSI model

In terms of soil structure interaction (SSI) analysis, the finite element method (FEM) is implemented to integrate respective elements, as defined by node response, thereby simulating the entire soil mass response. Even though soil structure interaction analysis presents some limitations, defined by ensuring accuracy in simulating the soil masses, the FEM technique represents some effective means of working through the limitations within defined physical limits.

Instead of trying to model extremely large volumes of soil, which would then be very computationally intensive, FEM enables efficient representation of the soil mass by keeping the number of elements, whether solids or nodes, within manageable size. This approach is computationally efficient with no significant compromising of the accuracy of the analysis.

The mechanical properties from Table 3 were used to develop the soil model by 8-point solid elements within the SAP2000 program. Figure 6 depicts the SSI model.

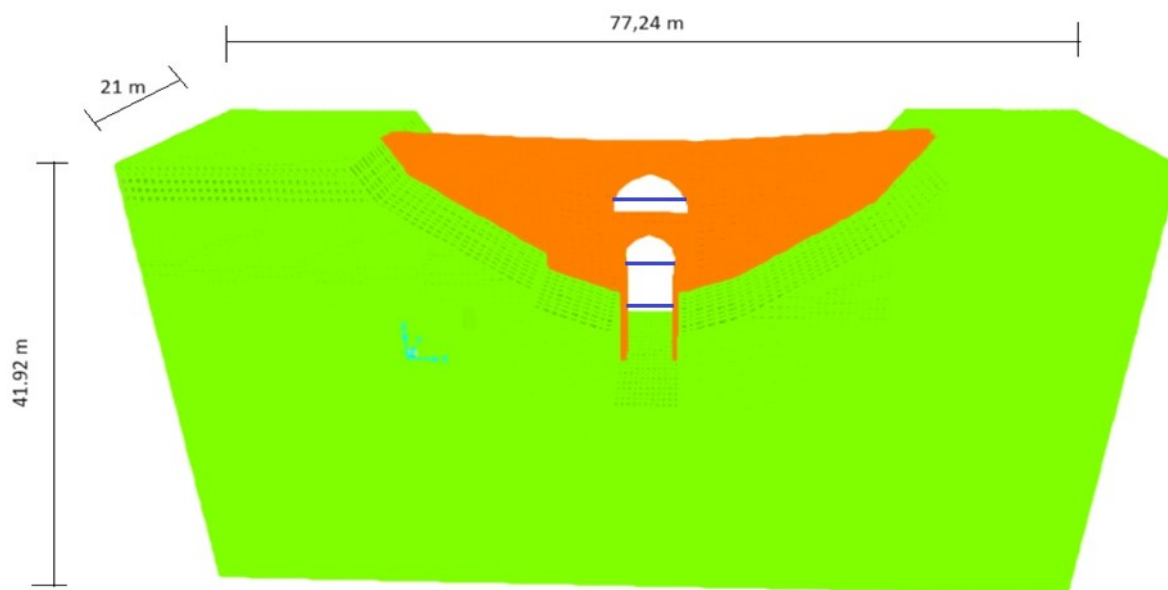


Figure 6: SSI model.

In the soil-structure interaction model, the dimensions of the soil were determined by examining the extant literature on the subject. The size ranges utilised by different researchers in the literature [25, 26] were evaluated, and the most appropriate limits were selected to ensure safety. In the bridge's SSI model 642615 solid elements and 682969 nodes were used. The FS model assumes that the bridge is fixed at the points where it connects with the ground. Conversely, the SSI model postulates that the ground can only translate in the z-direction at the side faces and is constrained in all three directions (x, y, z) at the base. It is assumed that there is full adherence between the structure and the ground. Damping ratios of $\xi_s=5\%$ and $\xi_f=7\%$ were selected for the bridge and foundation soil domains, respectively, based on literature [24].

This becomes more complex when SSI is taken into consideration in the analysis. Linear models with SSI can provide useful information on the dynamic behavior of the structure, as also observed in the current study where the consideration of SSI in the linear analysis of Cirimbolu Bridge provided significant in-sights into the displacement and stress distribution under seismic loading.

4.2 Determination of seismic parameters

In order to assess the seismic behaviour of the arch bridge, an analysis was conducted on the east-west components of the Pazarcık and Elbistan earthquakes that occurred in Kahramanmaraş on 6 February 2023. Earthquake codes define attenuation coefficients that take into account inelastic behavior according to the type of construction material and its ductility capacity. In this study, the earthquake load reduction coefficient ($R_a = 2.5$) defined in TBDY 2018 was used to consider inelastic behavior. The earthquake data for the DD-2 earthquake ground motion level, as defined in TBDY 2018 [16], was obtained from the Turkey Earthquake Hazard Map interactive web application [27] depending on the location of the arch bridge. Table 4 presents the obtained earthquake data. Table 5 presents the earthquake data required for seismic analysis, including peak ground acceleration (PGA), peak ground velocity (PGV), and torque magnitude (Mw).

The SeismoMatch program was employed to align the data pertaining to the region where the arch structure is situated, with a maximum period of 2 seconds and a minimum period of 0.01 seconds. The spectrum curves were generated with a damping ratio of 5%.

Table 4: Earthquake data [28]

Earthquake ground motion level	Local ground level	Ss	S1
DD2	ZB	0.619	0.149

Table 5: Earthquakes used in the analysis [28]

Parameter		Pazarcık	Elbistan
Mw		7.7	7.6
Vs30 (m/s)		484	543
Distance to the station (km)		25.6	17.7
PGA (g)	Original	0.56724	0.39949
PGV (cm/s)		127.4933	92.8431
PGA (g)	Matched	0.23123	0.30257
PGV (cm/s)		36.4298	46.1676
Station		Pazarcık	Nurhak

Figure 7 illustrates the original and paired response spectra obtained from the SeismoMatch program, while Figure 8 depicts the original and paired acceleration records. The analysis was conducted exclusively for the DD2 level, which was designated as the standard design earthquake ground motion in TBDY 2018.

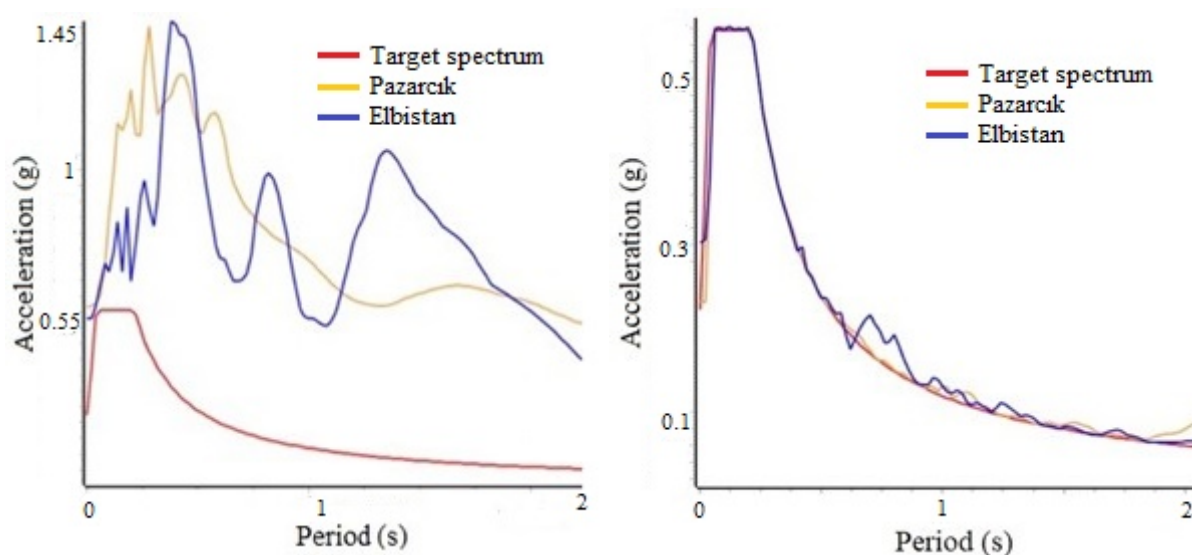


Figure 7: Original and matched spectrums

Upon examination of Figure 7, it becomes evident that the spectrum values of the Pazarcik and Elbistan earthquakes exceed the design spectrum values for the location of the building. Table 3 demonstrates a notable decline in PGA and PGV values following the matching of the acceleration records. For example, the peak ground acceleration (PGA) and peak ground velocity (PGV) values of the Pazarcik earthquake decreased by 59.3% and 71.4%, respectively, following the matching process.

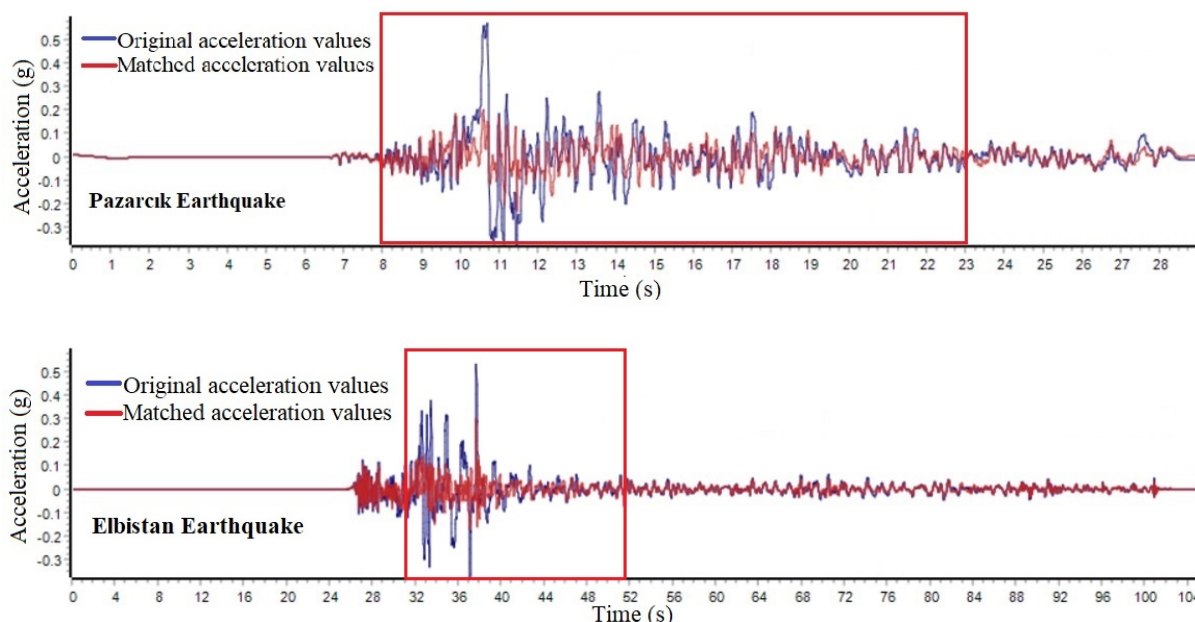


Figure 8: Original and matched acceleration time graphs of earthquakes

As illustrated in Figure 8, the 8-12 s and 30-50 s time periods of the Pazarcik and Elbistan earthquakes, respectively, were employed to reduce the analysis time.

5 Findings and discussion

5.1 Modal analysis

Mode shapes are of significant importance in the study of the general behaviour of bridges. The initial four mode shapes resulting from the modal analysis are presented in Figure 9. As illustrated in Figure 9, the mode shapes obtained in the FS and SSI models were found to be similar.

The FS model assumes a fully rigid connection between the structure and the ground, which is expected to result in lower period values. The modal analysis of the SSI model yielded lower frequency values, with a 7.1% decrease in the first mode frequency compared to the FS model. The findings align with those of previous studies conducted in the literature by [10, 11, 26]

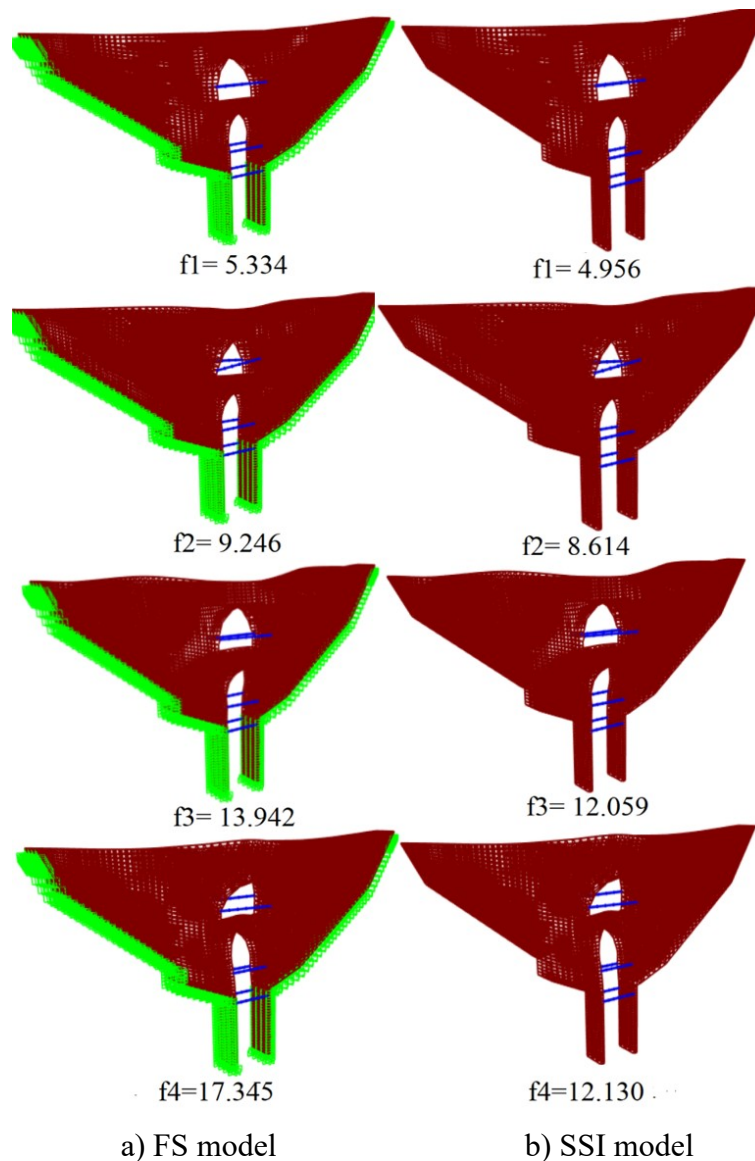


Figure 9: First 4 mode shapes and frequency values (Hz)

When the mode shapes obtained as a result of modal analyses are examined, it is observed that in both models, the first mode is dominated by the bending mode in the y-direction, while

the second mode is dominated by the torsional mode. However, in the SSI model, there is vertical movement in the 3rd and 4th modes, while in the Fixed model, the bending mode is dominant in the y-direction.

The mass participation ratios obtained as a result of modal analysis are shown in Table 6.

Table 6: Mass participation ratios

Mode	Fixed Model				SSI Model			
	Period (s)	Mass participation ratio			Period (s)	Mass participation ratio		
		X direction	Y direction	Z direction		X direction	Y direction	Z direction
1	0.188	0.000	0.435	0.000	0.202	0.000	0.010	0.000
2	0.108	0.000	0.435	0.000	0.116	0.000	0.010	0.000
3	0.072	0.000	0.472	0.000	0.083	0.000	0.010	0.731
4	0.058	0.000	0.646	0.000	0.082	0.002	0.010	0.739
5	0.055	0.000	0.646	0.000	0.077	0.002	0.011	0.739
150	0.008	0.909	0.924	0.895	0.011	0.832	0.807	0.934

A total of 150 modes were subjected to modal analysis within the scope of the study. Due to the substantial quantity of elements in the SSI model, it was only possible to perform modal analysis up to the 150th mode. Upon examination of Table 6, it was determined that there were significant differences in the mass participation ratios of the Fixed and SSI models. For instance, when the initial five modes were analysed, significant mass participation was observed in the y direction within the Fixed model, while the SSI model exhibited significant mass participation in the z direction, commencing from the third mode. In particular, while the third mode has a mass participation of 47.1% in the y-direction in the fixed model, the participation of this mode is quite low in the SSI model. This shows that SSI significantly changes the seismic behaviour and makes the structure behaviour more complex. Furthermore, an analysis of the 150th mode revealed that the Fixed model exhibited 90% mass participation in nearly all directions. In contrast, the SSI model exhibited mass participation exceeding 90% only in the Z direction.

Figure 10 shows position of first period values of bridge models in the design spectrum. Upon examination of Figure 10, it becomes evident that the bridge will be subjected to the highest acceleration values when the period value falls within the range of 0.08–0.2 s.

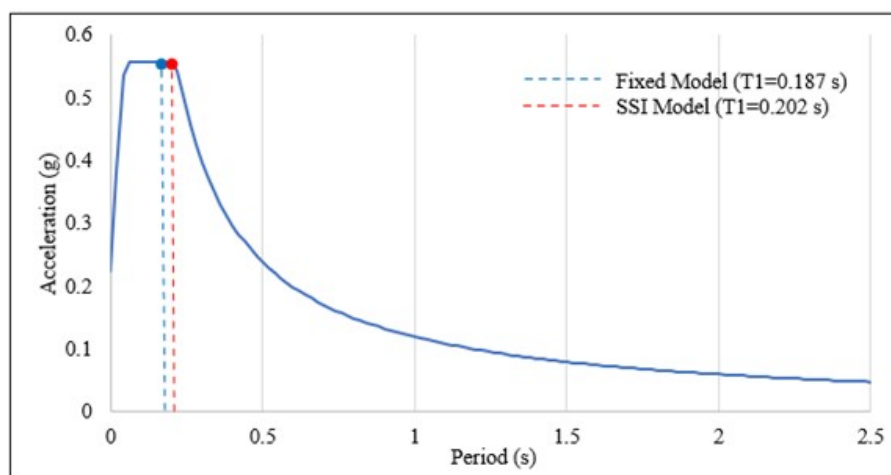


Figure 10: Position of first period values of bridge models in the design spectrum

5.2 Time history analysis

A linear time history analysis was conducted on the historical Cirimbolu bridge in the y direction (flow direction) using the acceleration records of the Pazarcık and Elbistan earthquakes that occurred on 6 February 2023. The results of the analysis were examined separately for each earthquake loading.

Figure 11 presents a graph of the displacement at the peak as a function of time. Figure 12 illustrates the displacement of the bridge as a function of height in the y direction. Additionally, the peak point on the model is marked with a star.

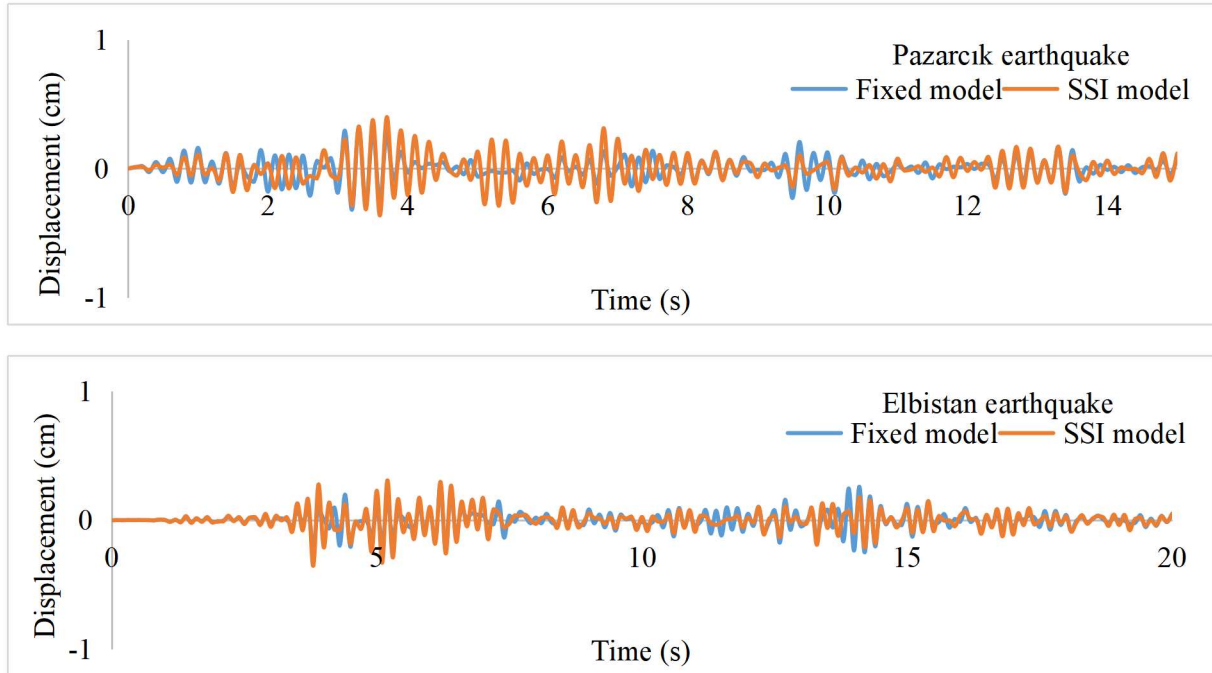


Figure 11: Displacement time graph of the peak point

Upon examination of Figure 12, it can be observed that regardless of earthquake loading, displacements exhibited a nonlinear increase in height, reaching a maximum value at the peak. Similarly, in the studies conducted in the literature, it was determined that the highest displacement values occurred at the upper part of the arch and at the top point of the bridge. [4, 29].

In Figures 11 and 12, the greatest displacements observed were 3.2 mm and 2.7 mm, respectively, in the Fixed model, in response to the Pazarcık and Elbistan earthquakes. In the SSI model, the largest displacements were 4 mm and 3.5 mm for the Pazarcık and Elbistan earthquakes, respectively. The time-history analyses conducted on both models revealed that the highest displacement values were caused by the Pazarcık earthquake loading.

Figures 11 and 12 illustrate the impact of boundary conditions on the displacement values of the bridge. The time history analysis revealed that the displacement values were higher for both earthquake loadings in the SSI model. A comparison of the highest displacement values of the Fixed model and SSI models reveals an increase of 25% and 29.6% in the SSI model for the Pazarcık and Elbistan earthquakes, respectively. Additionally, studies in the literature have yielded comparable results [11, 26]

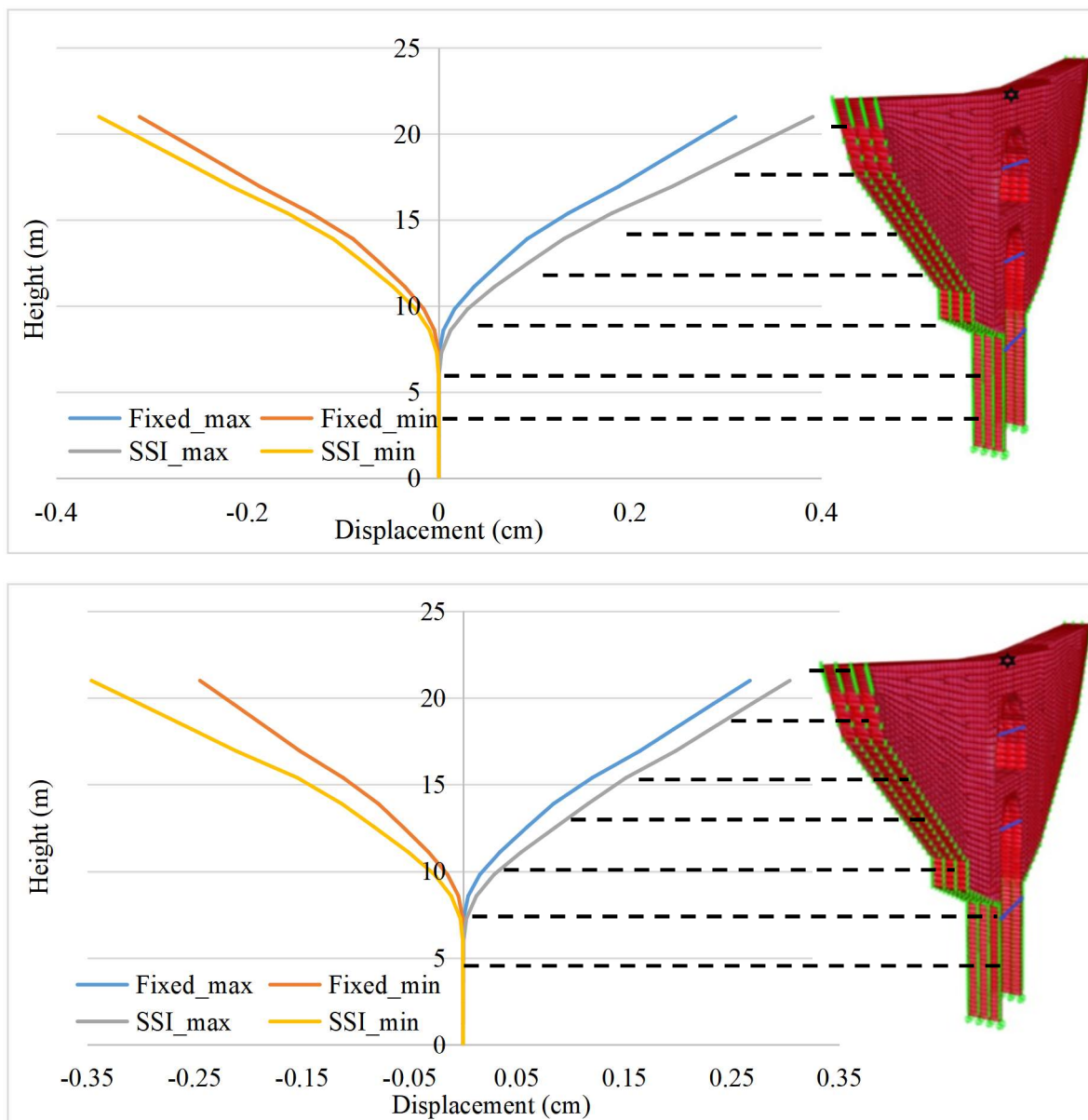


Figure 12: Displacements that vary depending on altitude.

Table 7 presents the stress values resulting from time history analyses in both models, along with the percentage increase in stress values observed in the SSI model relative to the Fixed model.

Table 7: Maximum stresses resulting from time history analysis.

Stress	FS model		SSI model		Increase (%)	
	Pazarcık	Elbistan	Pazarcık	Elbistan	Pazarcık	Elbistan
Tensile (kPa)	412	351	480	359	14.2	2.2
Compressive (kPa)	424	323	447	455	5.1	29
Shear (kPa)	79	75	86	80	8.1	6.25
Smax (kPa)	502	447	608	537	17.4	16.7
Smin (kPa)	483	429	520	522	7.1	17.8

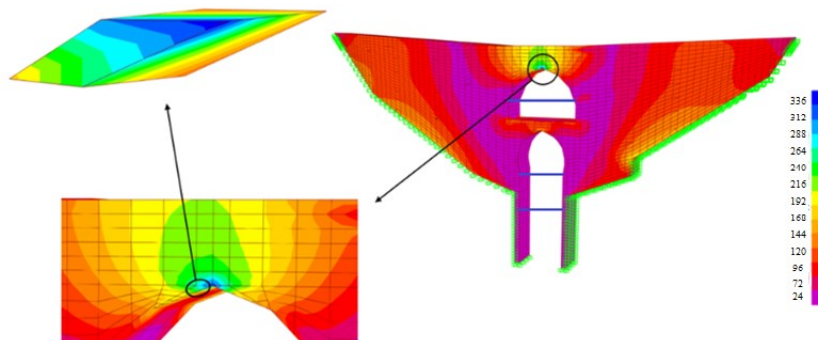
Upon examination of Table 6, it becomes evident that the highest stress values for both models were obtained from the Pazarcık earthquake loading. Upon comparison of the effects of boundary conditions, it was determined that the SSI model yielded higher stress values. For instance, when comparing the largest value of maximum principal stresses, an increase of 17.4% and 16.7% occurred for the Pazarcık and Elbistan earthquakes, respectively, in the SSI model.

The safety stress values of the materials presented in Table 2 were compared with the stress values obtained as a result of the time history analyses presented in Table 6. Upon examination of the stresses occurring on the bridge, it was determined that the tensile safety stress was exceeded, while the pressure and shear safety stresses were not exceeded.

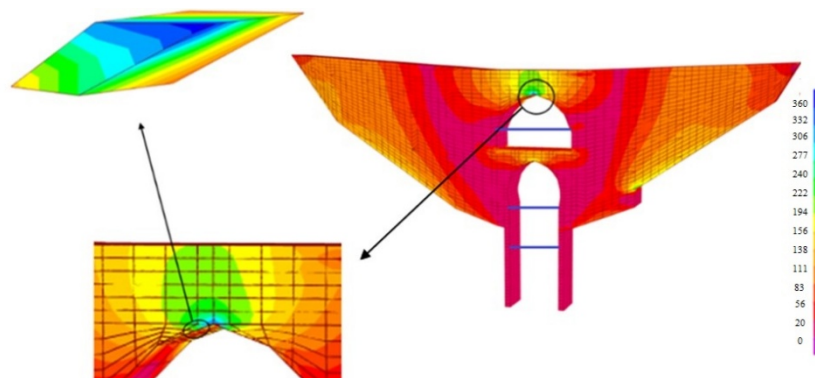
Diagrams of normal stress, comparable to those observed during the Pazarcık earthquake loading, were also observed during the Elbistan earthquake loading. Figure 13 displays the normal stress contours for the Elbistan earthquake loading in both models resulting from time history analysis, highlighting the solid element with the highest normal stress.

Upon examination of Figure 13, it becomes evident that the distribution of normal stresses is similar in both models, with the highest concentrations occurring in analogous regions. The highest normal stresses were observed in the upper parts of the arch in both models, occurring in the same solid element.

The shear stress diagrams were also found to be similar due to the loading of the Pazarcık and Elbistan earthquakes. The results of the time history analysis are presented in Figures 14 and 15, which display the shear stress contours for the Pazarcık and Elbistan earthquake loadings, respectively. The solid elements in which the largest shear stress was observed in both models are also shown.

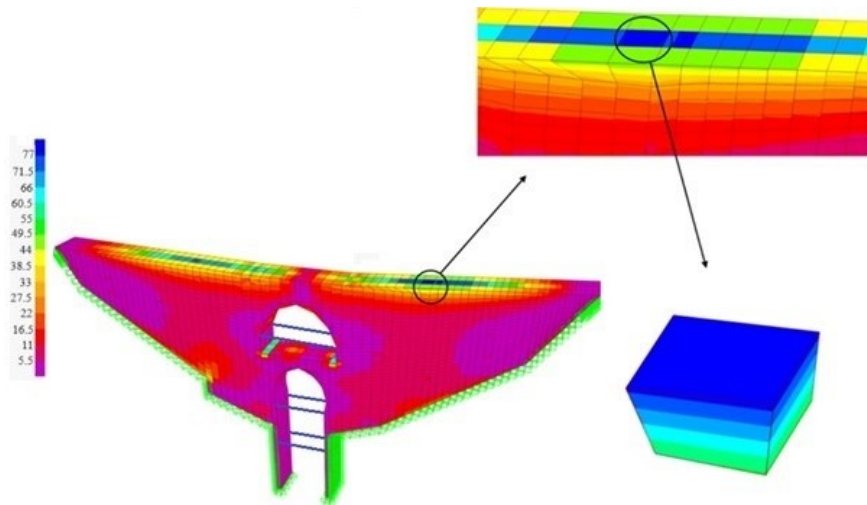


a) FS model

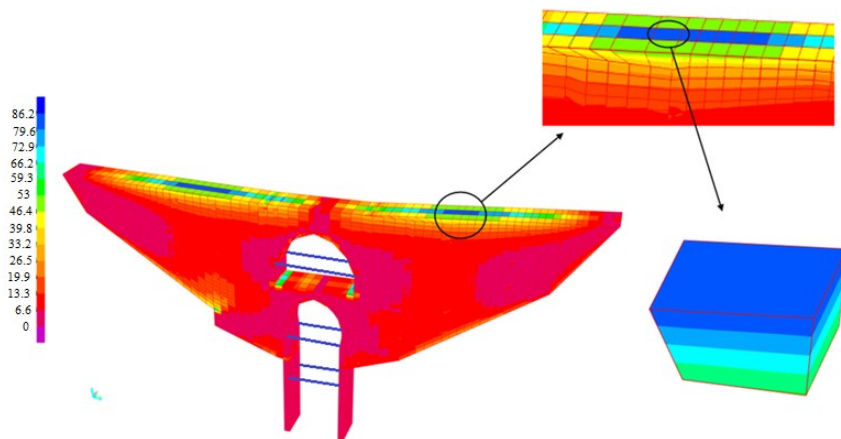


b) SSI model

Figure 13: Normal stress contours for Elbistan earthquake (kPa).

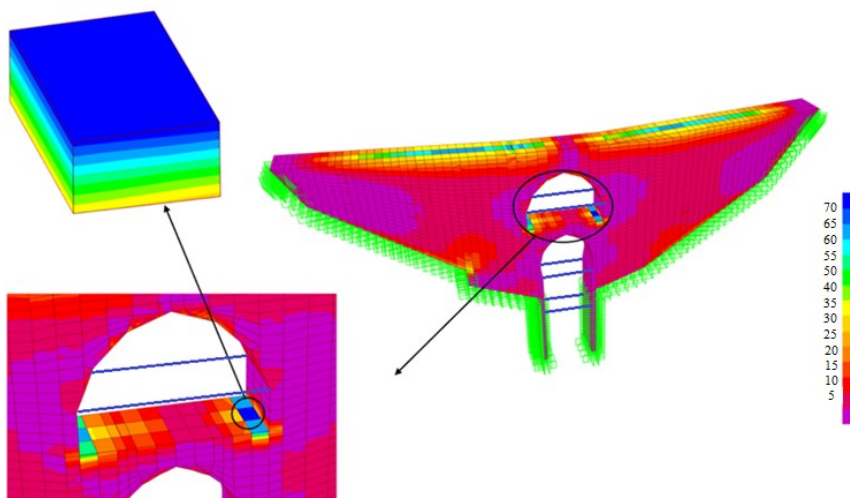


a) FS model

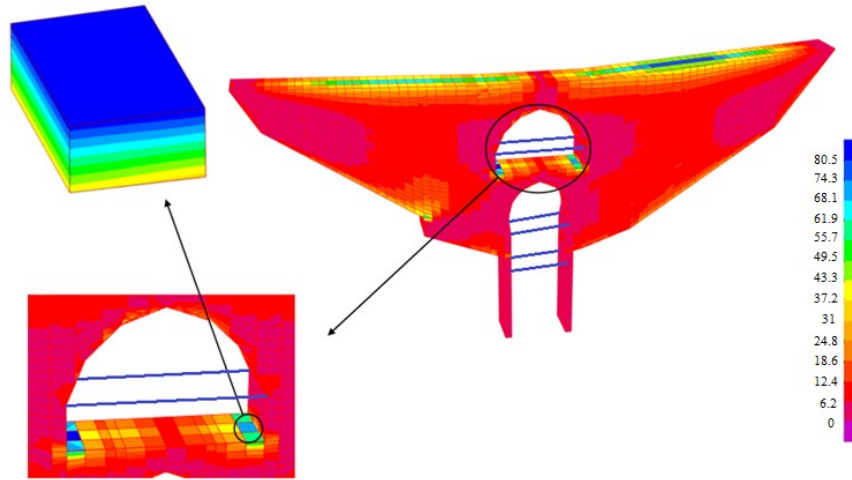


b) SSI model

Figure 14: Shear stress contours for Pazarcik earthquake (kPa).



a) FS model

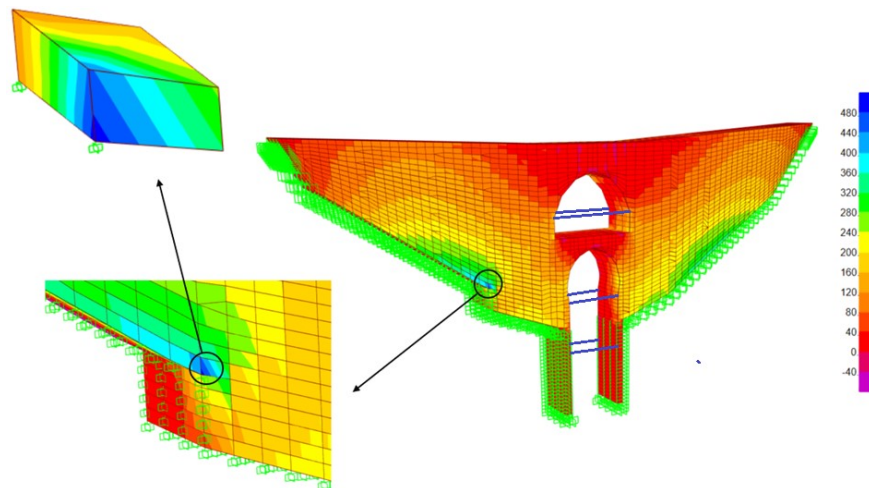


b) SSI model

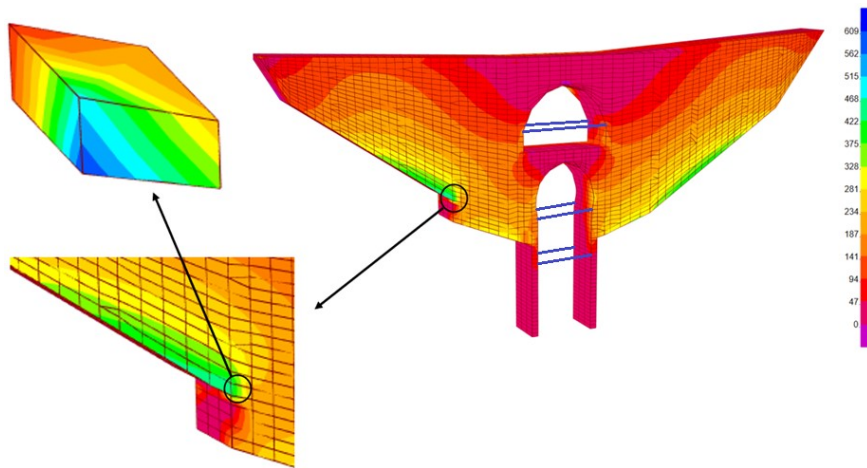
Figure 15: Shear stress contours for Elbistan earthquake (kPa).

Upon examination of Figures 14 and 15, it becomes evident that shear stresses are concentrated in similar regions in both models. In the Pazarcık earthquake, the highest shear stresses were observed on the upper surface of the bridge in both models (The same solid element experienced the highest stresses in both models). Similarly, in the Elbistan earthquake, the largest shear stresses were observed in the upper parts of the lower arch (the same solid element experienced the highest stresses).

Analogous maximum and minimum principal stress diagrams were observed as a consequence of the Pazarcık and Elbistan earthquake loading. Figures 16 and 17 illustrate the maximum and minimum principal stress contours, respectively, for the Pazarcık earthquake loading in both models as a result of time history analysis. The solid elements in which the largest principal stress occurs are also displayed.

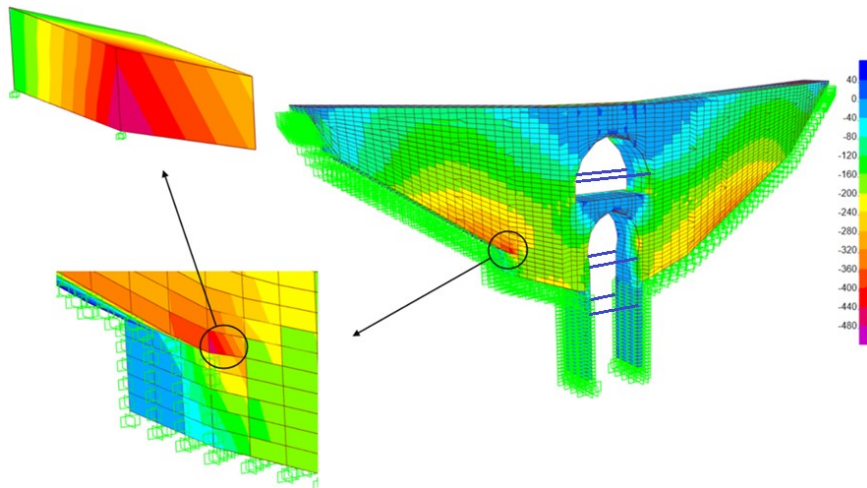


a) FS model

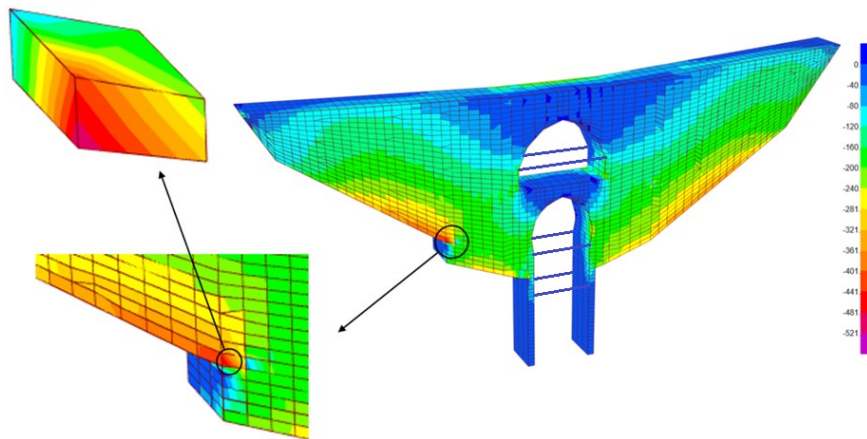


b) SSI model

Figure 16: Maximum principal stress contours (kPa).



a) Fixed model



b) SSI model

Figure 17: Minimum principal stress contours for Pazarcik earthquake (kPa).

Upon examination of Figures 16 and 17, it becomes evident that both models exhibit the concentration of maximum and minimum principal stresses in analogous regions. The highest values of maximum principal stresses have been observed in the same solid element where the bridge makes contact with the ground in both models. Previous studies in the literature have yielded similar results [3, 30].

6 Reinforcement suggestions for historical Cirimbolu Bridge

Following the implementation of two distinct analytical models, namely seismic analysis and visual inspections, it was established that the central piers and arches represent the most susceptible structural elements of the historical bridge. In order to ensure the sustainability of the structure and the safety of pedestrians and light vehicles during seismic events, strengthening strategies have been proposed.

6.1 Material reinforcement

The initial recommendation is to replace the stones in order to reinforce the arch and foot sections of the historic structure (see Figure 18). This method involves the replacement or reinforcement of the existing materials used in the bridge with modern, more durable materials. For example, the use of high-strength concrete or steel reinforcements can be employed to reinforce old stone masonry. In order to maintain the consistency and originality of the historical building during reinforcement, high-strength mortars will be employed to mount the same stone material. In this instance, lime mortar with a compressive strength of at least 3.5 MPa will be utilised.

Furthermore, a finite element model will be developed by modifying the material properties of the arches and central pillar. In order to reinforce the bridge piers, it is necessary to remove the vegetation around the edges and replace the stones with those that have been bound together with a 0.7 m deep lime mortar.

The elasticity modulus of the wall was calculated to be 4730 MPa using Equation (2), which takes into account the mechanical properties of the stone and mortar. In calculating the elasticity modulus of the wall, we assumed a factor of 400 times f_c .

$$f_c = 0.6f_b^{0.65}f_m^{0.35} \quad (2)$$

In this equation;
 soft mortar with compressive strength (f_m)
 compressive strength of stone (f_b)

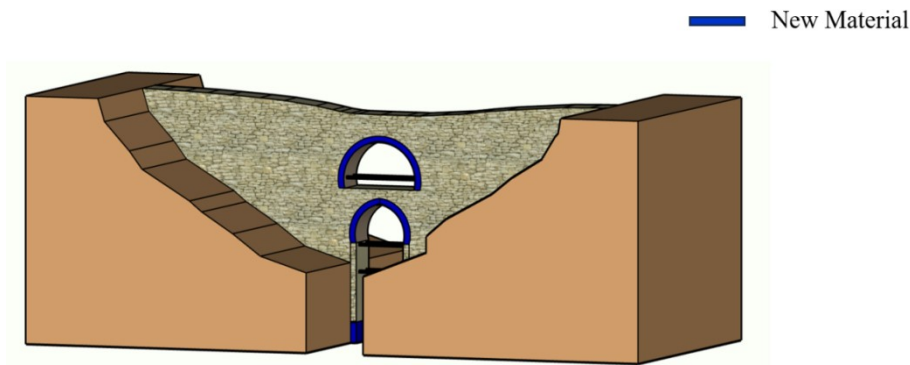


Figure 18: Reinforcement with new material (source: authors).

6.2 Reinforcement with CFRP elements

Fiber-reinforced polymer (FRP) composites are extensively used due to their low specific gravity, corrosion resistance, high tensile strength, strong adaptability to curved surfaces, and ease of application. Studies have shown that reinforcing the back or bottom of a masonry arch with FRP greatly increases its carrying capacity and ductility. It is important to note that FRP materials are not suitable for use on wet surfaces or in low temperatures. In order to ensure the correct adhesion of the FRP element to the base material, it is necessary to create a smooth surface. In the event that the surface of the historical bridge is too rough, this may have a detrimental effect on the adhesion of the epoxy resin. Consequently, the lower base of the arch inner section will be prepared and reinforced prior to the application of FRP. Given the likelihood of water leakage at the base of the bridge, it is not advisable to add FRP to this section. This is because it would accelerate the deterioration of FRP, as noted by Garmendia et al. [31], and Alecci et al. [32].

The CFRP material properties selected were a modulus of elasticity of 230,000 MPa, unit volume weight of 1,760 kg/m³, one-way sheet knitting shape, and a thickness of 0.131, as reported by Altunışık [33]. Similar to the studies in the literature, the CFRP material was modeled as a shell element [34]. The strengthening carried out using CFRP is illustrated in Figure 19.

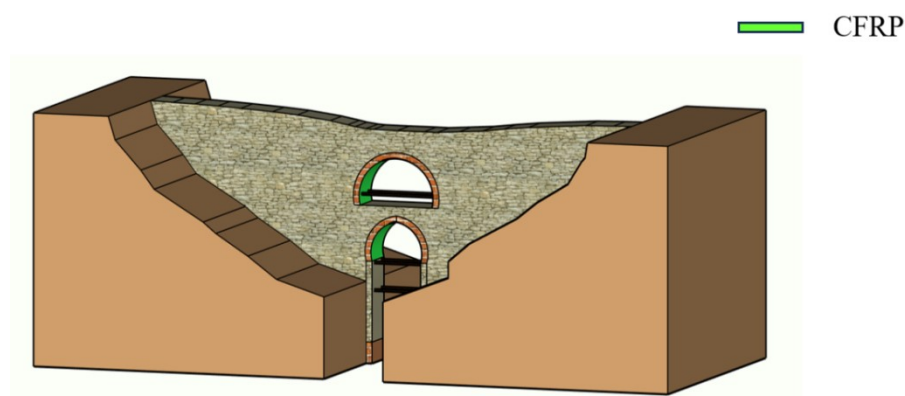


Figure 19: Reinforcement with CFRP material (source: authors)

6.3 Reinforcement with FRCM composite

The bonding ability of these materials is enhanced by the fact that both the matrix mortar and walls are inorganic materials. These materials can be applied to rough and wet surfaces, exhibit good resistance to high temperatures, and can overcome the irreversible shortcomings of inorganic adhesives [2]. In practice, it is assumed that there is a perfect bond between the FRCM layers and the wall. In the context of strengthening techniques utilising FRCM, it is recommended that the abutments of historical bridges be reinforced with an FRCM composite layer. This will result in the walls becoming more ductile and increasing their deformation capacity. Furthermore, a salt-resistant hydraulic binder based on lime and eco-pozolan should be injected into the wall during cladding with FRCM composite.

The FRCM composite was modelled using material properties of 10,000 MPa for Modulus of Elasticity, 1900 kg/m³ for Density, and 2.67 MPa for Tensile Strength. The thickness of FRCM was set at 4 cm, as reported by Bayraktar and Hokelekli [35]. Similar to the studies in the literature, the FRCM material was modeled as a shell element [2]. The strengthening carried out using FRCM is illustrated in Figure 20.

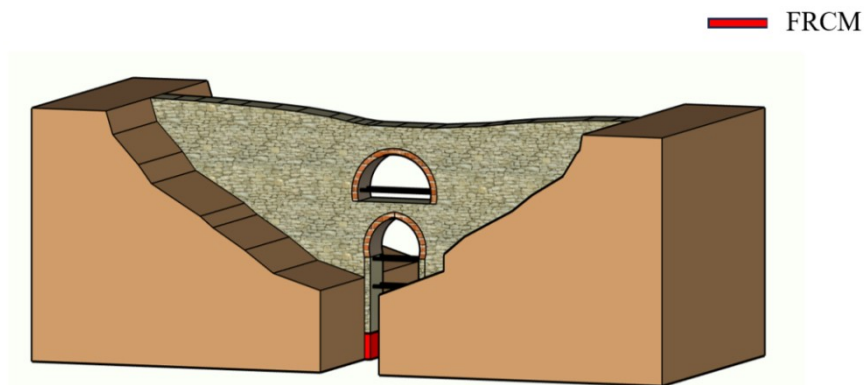


Figure 20: Reinforcement with FRCM (source: authors).

6.4 Renewal of tension rods for arch beams

The use of tension elements in the arches of historical bridges reinforces the original architecture while improving durability. Typically, in the form of steel cables or reinforced concrete bars, these elements are placed on the top part of the bridge arch to enhance its load-bearing capacity.

A review of historical structures, including mosques, inns, baths, madrasahs, caravanserais, and churches that have survived from the Ottoman and Roman periods to the present day, particularly in Anatolia, reveals the use of iron tension rod systems in the arches from the column-arch junction areas. The use of iron tension rod systems is of critical importance in maintaining the structural stability of the arch. The lateral openings at the arch abutments are prevented from occurring under vertical load, thereby increasing the strength of the arch. Tension elements are mounted on both sides of the arch and anchored to it using steel anchors or reinforced concrete blocks. The tension in the elements is calibrated to the bridge's geometry and requirements through the application of a specific force. It is recommended that the wooden beams currently in use at the Cirimbolu Bridge be replaced with steel beams.

When modelling steel tension rods, material properties such as the elastic modulus (203704 MPa) and Poisson's ratio (0.3) are taken into account [36]. Figure 21 illustrates the strengthening carried out using steel strips.

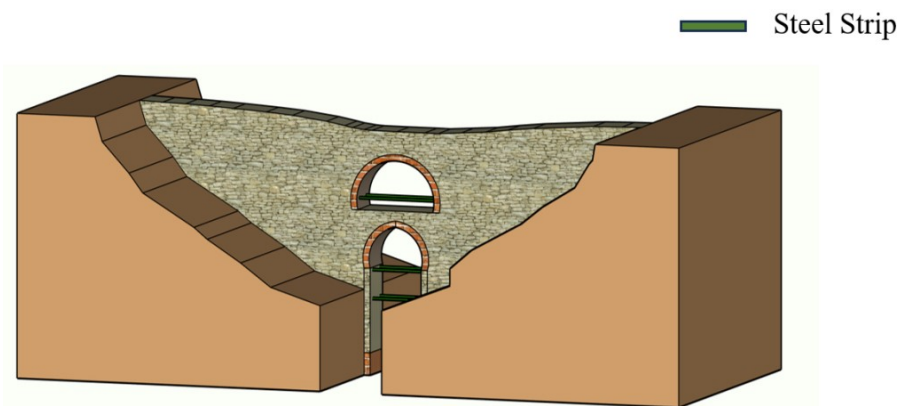


Figure 21: Reinforcement with steel strip (source: Authors)

6.5 Evaluation of reinforcements

In the SAP2000 computer program, three new models have been created according to the reinforcement methods previously mentioned. These models represent steel tension, CFRP, and FRCM. Linear time history analyses have been conducted on the aforementioned models. The largest displacements obtained from the aforementioned analyses have been compared. Figure 22 illustrate the maximum displacements obtained from the models. Figure 23 shows the reductions in displacement following the application of strengthening methods.

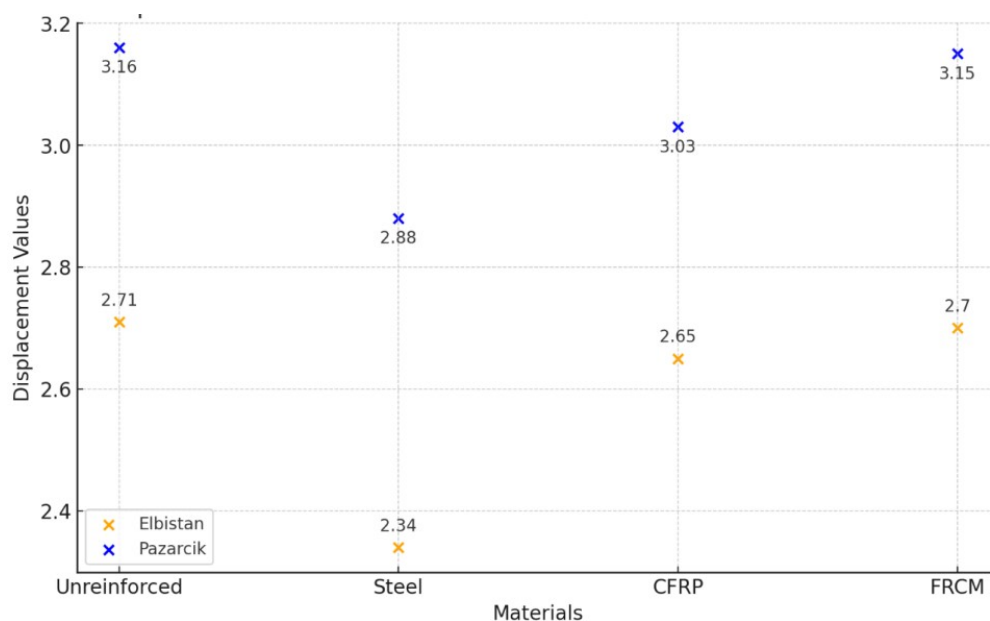


Figure 22: Displacemet values of different models in Elbistan and Pazarcık.

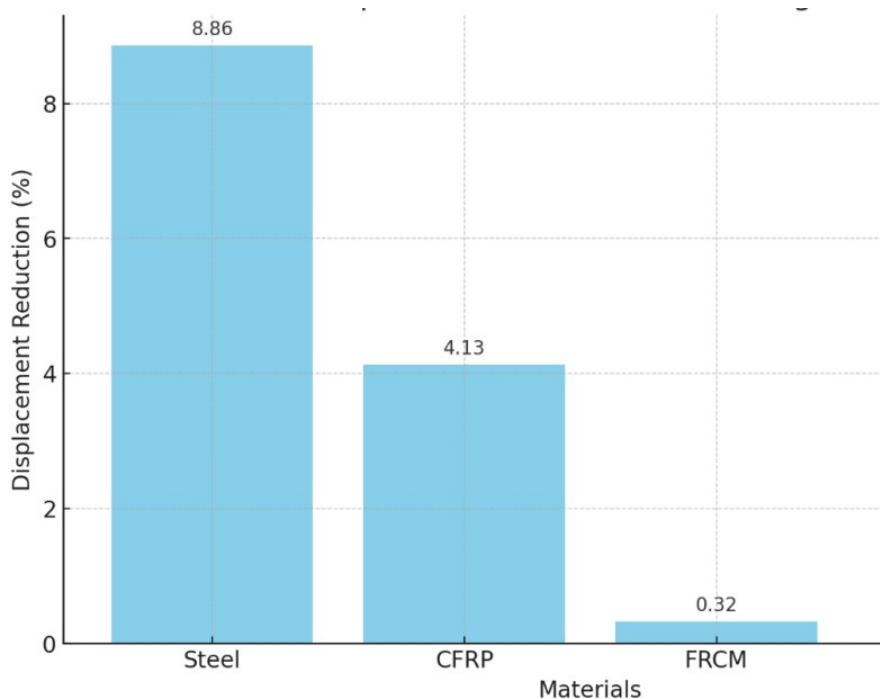


Figure 23: Reduction in displacement values with strengtning methods.

Figure 22 shows that the unreinforced model had the highest displacement. However, the displacement values exhibited a reduction when the models were reinforced. For example, in Figure 23, when the Pazarcık earthquake load is applied, it is seen that there is a decrease of 8.86%, 4.13% and 0.32% in the displacement values of the steel, CFRP and FRCM reinforced models compared to the unreinforced model, respectively. The study concluded that the most effective reinforcement method is the use of steel tendons in place of wooden tendons. The application of FRCM for reinforcement resulted in minimal changes to the displacements. This indicates that the FRCM application was insufficient to enhance the bridge's strength. Consequently, it is recommended that if this reinforcement method is preferred, FRCM should be applied to a greater extent across the bridge. Table 8 presents the statistical analysis of displacement values for each model type.

Table 8: Statistical Analysis for each strengthening material.

Material	Mean	Std	Min	25%	50% (Median)	75%	Max
FRCM	2.925	0.318	2.70	2.8125	2.925	3.0375	3.15
CFRP	2.840	0.269	2.65	2.745	2.840	2.935	3.03
Steel	2.610	0.382	2.34	2.475	2.610	2.745	2.88
Unreinforced	2.935	0.318	2.71	2.8225	2.935	3.0475	3.16

A review of the extant literature revealed that the deformation-reducing effect of CFRP yielded results consistent with the hypothesis. This finding led to the conclusion that such reinforcement methods are effective in increasing the durability of masonry bridges.

To statistically evaluate the differences among the strengthening methods, an analysis of variance (ANOVA) was conducted. The ANOVA results indicated an F-statistic of 6.30 and a p-value of 0.005. Since the p-value is below the 0.05 significance threshold, it can be concluded that there are statistically significant differences in the displacement means among the strengthening methods (FRCM, CFRP, Steel, and Unreinforced). These findings substantiate the conclusions regarding the effectiveness of the applied strengthening techniques.

A detailed statistical summary of the displacement values for the strengthened and unreinforced models is presented in Table 7. This summary includes the mean, standard deviation, minimum, maximum, and percentile values (25%, 50% or median, and 75%). The mean values represent the typical performance of each strengthening method. For instance, the unreinforced model exhibits the highest average displacement value (2.935), indicating that it is less stable compared to the strengthened models. The maximum displacement values for FRCM (3.15) and the unreinforced model (3.16) are notably higher than those observed for other methods, suggesting a greater displacement capacity in these cases. Additionally, the percentile values provide further insights into the data distribution, with the median values confirming a symmetrical distribution. These results clearly highlight the superior effectiveness of the steel-reinforced model in reducing displacements, while FRCM reinforcement yields negligible changes in displacement values.

Figure 24 shows the base shear forces obtained as a result of time history analysis.

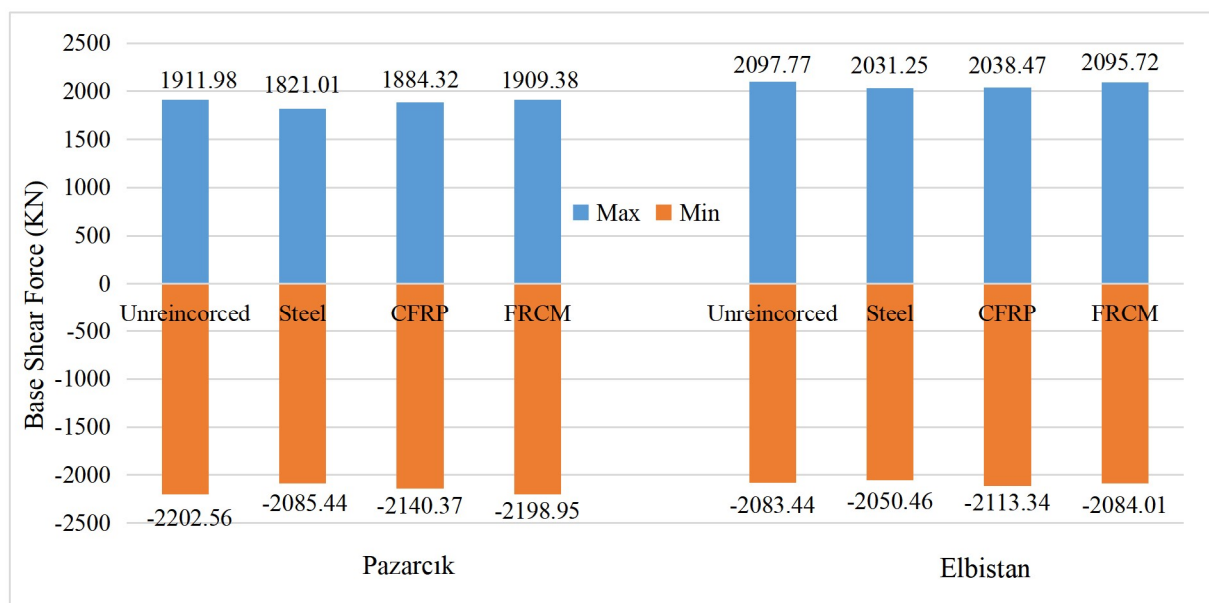


Figure 24: Base shear forces.

Based on the examination carried out on Figure 24, it is noted that the unreinforced model had the greatest base shear force under the impact of both earthquake loading cases. On the other hand, the model placed with the reinforcement method using steel bars was noted to have the least base shear forces. It is noted that the base shear forces of the model using the reinforcement method involving FRCM are located near the base shear forces of the unreinforced model. Upon examination of the reinforcement methods, with emphasis on the base shear forces triggered, it is noted that the most efficient method is the reinforcement method using steel bars.

The performance of all the reinforcement methods for the historical bridge, steel tendons, CFRP, and FRCM, was examined, comparing them. The result was that steel tendons proved useful, while FRCM was found to have little impact in reducing displacement.

These are the main reasons for the low effectiveness of FRCM: its stiffness is lower than that of steel tendons and CFRP. In addition, in the present study, FRCM was applied only in some critical areas, limiting its effectiveness in enhancing the overall structural behaviour of the bridge. In the next steps, FRCM effectiveness will be investigated by increasing its application area and changing the binding material.

Besides, reinforcement performance due to CFRP can be influenced by environmental factors. As it is well known, the sensitivity of CFRP to moisture and temperature variation is high, especially because of epoxy-based adhesives. This fact is of great relevance to the long-term durability of CFRP in historical masonry bridges that are inclined to retain moisture. Therefore, surface preparation in CFRP applications must be made very carefully, and techniques against moisture must be applied. Since this study was performed only by numerical analyses, further studies should be performed to investigate the effects of environmental factors on the long-term performance of CFRPs in historical bridges in more detail.

Therefore, for historical bridges, seismic strengthening should be done with materials selected considering not just mechanical properties, but also their resistance to environmental effects. It is finally suggested that future research studies include experimental and nonlinear analyses as well, in order to have an all-around study of the long-term performance of reinforcement methods.

7 Conclusion

The evaluation aimed at exploring the impacts of specified conditions on seismic action on the behavior of an arch bridge during a seismic event, using the old Cirimbolu Bridge in Isparta as an existing case. The evaluation used the SAP 2000 programming program, creating two finite element modules. The modules were designed with specifications reflecting conditions where a bridge is fixed on the ground, as well as specifications reflecting conditions on the ground. The analysis performed by these modules is as discussed in more detail in this report. A comparison of the seismic records of the Pazarcık and Elbistan earthquakes with the seismicity of the region where the historical Cirimbolu Bridge is located revealed a significant decrease in the peak ground acceleration (PGA) and peak ground velocity (PGV) values.

1. The results of the modal analysis indicated that the SSI (Soil-Structure Interaction) model exhibited higher frequency values when compared to the Fixed model.

2. The SSI model exhibited a 7.1% reduction in frequency values in comparison to the Fixed model when the first modes were considered.

3. In both models, the highest displacement values were observed at the peak points, irrespective of the earthquake loading.

4. The Pazarcık earthquake loading resulted in the highest displacement values for both models in the time history analyses.

5. The highest normal stress, shear stress, and maximum and minimum principal stresses were obtained from the Pazarcık earthquake loading in the time history analyses for both models.

6. A comparison of the effects of boundary conditions revealed that the SSI model yielded higher stress values for normal stress, shear stress, and maximum and minimum principal stresses.

7. In both the Fixed and SSI models, the normal stresses reached their highest values at the upper portions of the arch for both earthquake loadings.

8. In both the Fixed and SSI models, the shear stresses were concentrated at the top surface of the bridge and the upper surface of the underlying arch for the Pazarcık and Elbistan earthquake loadings.

9. Furthermore, the maximum and minimum principal stresses reached their highest values at the regions where the bridge contacts the ground for both earthquake loadings.

10. Upon examination of all stress diagrams, it was observed that stresses were concentrated in the same regions, regardless of boundary conditions.

11. Upon examination of the stresses occurring on the bridge, it was determined that the tensile safety stress was exceeded, while the pressure and shear safety stresses were not exceeded.

12. The use of steel tendons was determined to be the most effective reinforcement method, in comparison to wooden tendons.

13. When reinforced with FRCM, the displacements remained almost unchanged.

14. A comparison of the reinforcement methods in terms of base shear forces revealed that the most effective method was reinforcement with steel bars.

This can be seen as a result of what had been explained in previous cases in reference to this same issue in terms of application to the case of the Cirimbolu Bridge, as it can offer a precise evaluation of its seismic behavior, specifically in reference to such structures as are historical in nature. Further, it can be of particular importance to conducting enhanced levels of increased protection as well as durability within a context such as a seismic activity occurrence. Along with this, there seems to be a better perspective on seismic behavior with

reference to reinforcement in terms of application to the same issue in reference to this case as a result of what has been researched.

Data Availability Statement

The numerical models and analysis results generated during this study are available from the corresponding author upon reasonable request.

Funding Statement

This research did not receive any specific grant from funding agencies in the public, commercial, or not-for-profit sectors.

Author contributions

Author 1: Writing the article and evaluating the results, Author 2: Writing the article and performing the analyses, Author 3: Writing the article and performing the analyses, Author 4: Collecting information about the bridge

Conflicts of interest

There is no conflict of interest in this study.

References

- [1] Kader, A., Sayın, E., & Özmen, A. (2021). Farklı sönüm tipleri altında tarihi yığma köprülerin sismik tepkilerinin değerlendirilmesi. *Fırat Üniversitesi Mühendislik Bilimleri Dergisi*, 34(1), 45-59.
- [2] Shabani, A., Kioumarsi, M., & Plevris, V. (2023). Performance-based seismic assessment of a historical masonry arch bridge: Effect of pulse-like excitations. *Frontiers of Structural and Civil Engineering*, 17(6), 855-869.
- [3] Sakcalı, G. B., Gönül, A., & Yüksel, İ. (2019). Seismic behavior of historical masonry bridges: The case study of Irgandi Bridge. *International Journal*, 6, 25.
- [4] Yılmaz, E. G., Sayın, E., & Özmen, A. (2022). Dynamic analysis of historical masonry arch bridges under different earthquakes: The case of Murat Bey Bridge. *Turkish Journal of Science & Technology*, 17(2), 461-473.
- [5] Sözen, Ş., & Çavuş, M. (2020). Tek açıklıklı tarihi taş köprülerde form değişikliğinin köprünün sismik davranışına etkisinin değerlendirilmesi: Niksar Yılanlı (Leylekli) Köprü örneği. *Düzce Üniversitesi Bilim ve Teknoloji Dergisi*, 8(1), 48-59.
- [6] Wolf, J. P. (1989). Soil-structure-interaction analysis in time domain. *Nuclear Engineering and Design*, 111, 381-393.

- [7] Kramer, S. L. (1996). Geotechnical earthquake engineering. Pearson Education India.
- [8] Ouanani, M., & Tiliouine, B. (2015). Effects of foundation soil stiffness on the 3-D modal characteristics and seismic response of a highway bridge. *KSCE Journal of Civil Engineering*, 19, 1009-1023.
- [9] Zani, G., Martinelli, P., Galli, A., Gentile, C., & di Prisco, M. (2019). Seismic assessment of a 14th-century stone arch bridge: Role of soil–structure interaction. *Journal of Bridge Engineering*, 24(7), 05019008.
- [10] Güllü, H., & Jaf, H. S. (2016). Full 3D nonlinear time history analysis of dynamic soil–structure interaction for a historical masonry arch bridge. *Environmental Earth Sciences*, 75, 1-17.
- [11] Özmen, A., & Sayın, E. (2023). 3D soil structure interaction effects on the seismic behavior of single span historical masonry bridge. *Geotechnical and Geological Engineering*, 41(3), 2023-2041.
- [12] Awlla, H. A., Taher, N. R., Aksoy, H. S., & Qadir, A. J. (2022). Effect of SSI and fixed-base concept on the dynamic responses of masonry bridge structures, Dalal Bridge as a case study. *Academic Journal of Nawroz University*, 11(3), 89-99.
- [13] Rovithis, E. N., & Pitilakis, K. D. (2016). Seismic assessment and retrofitting measures of a historic stone masonry bridge. *Earthquakes and Structures*, 10(3), 645-667.
- [14] TEC2007. Türkiye Bina Deprem Yönetmeliği; AFAD, 2007
- [15] Uysal, N., Usta, P., & Bozdağ, Ö. (2022). Structural resistance of a reinforced concrete building under earthquake and wind loads in Isparta and Burdur region. *Türk Doğa ve Fen Dergisi*, 11(1), 142-150. <https://doi.org/10.46810/tdfd.1060359>
- [16] TBDY2018. Türkiye Bina Deprem Yönetmeliği; AFAD, 2018
- [17] Şişik, Ö. (2017). Edirne'de bulunan 15. yy ve 16. yyda inşa edilmiş tarihi cami ve türbelerin taşıyıcı sistem analizi ve çözüm önerileri (Master's thesis, Selçuk University, Turkey).
- [18] GÜDÜ, D. (2021). Ahşap minarelerin taşıyıcı sistem özellikleri ve deprem davranışlarının incelenmesi (Doctoral Thesis, Bursa Uludağ University, Turkey)
- [19] Shabani, A., & Kioumarsı, M. (2023). Seismic assessment and strengthening of a historical masonry bridge considering soil-structure interaction. *Engineering Structures*, 293, 116589.
- [20] Lourenco, P. B. (1996). Computational strategy for masonry structures. Delft University of Technology and DIANA Research.
- [21] Özmen, A., & Sayın, E. (2020). Tarihi yığma bir köprünün deprem davranışının değerlendirilmesi. *Niğde Ömer Halisdemir Üniversitesi Mühendislik Bilimleri Dergisi*, 9(2), 956-965.

- [22] Giordano, A., Mele, E., & De Luca, A. (2002). Modeling of historical masonry structures: comparison of different approaches through a case study. *Engineering Structures*, 24(8), 1057-1069.
- [23] Roca, P., Cervera, M., Gariup, G., & Pelà, L. (2010). Structural analysis of masonry historical constructions. Classical and advanced approaches. *Archives of Computational Methods in Engineering*, 17, 299-325.
- [24] Bayraktar, A., & Hökelekli, E. (2021). Nonlinear soil deformability effects on the seismic damage mechanisms of brick and stone masonry arch bridges. *International Journal of Damage Mechanics*, 30(3), 431-452.
- [25] Hökelekli, E. (2020). Yapı-Zemin Etkileşiminin Tarihi Yığma Minarelerin Deprem Davranışına Etkisi. *Dicle Üniversitesi Mühendislik Fakültesi Mühendislik Dergisi*, 11(2), 825-838.
- [26] Lazizi, A. H., & Tahghighi, H. (2023). Influence of soil–structure interaction on seismic demands of historic masonry structure of Kashan Grand Bazaar. *Bulletin of Earthquake Engineering*, 21(1), 151-176.
- [27] Afet ve Acil Durum Yönetimi Başkanlığı. Deprem Tehlike Haritaları İnteraktif Web Uygulaması; 2025.
- [28] AFAD, Earthquake database. Retrieved January 15, 2024, from <https://earthquakedatabase.com/>
- [29] Nematlu, Ö. F., Güzel, İ., Balun, B., Öztürk, M., & Sarı, A. (2023). Nonlinear seismic assessment of historical masonry Karaz bridge under different ground motion records. *Bitlis Eren Üniversitesi Fen Bilimleri Dergisi*, 12(1), 247-260.
- [30] Özmen, A., & Sayın, E. (2021). Seismic response of a historical masonry bridge under near and far-fault ground motions. *Periodica Polytechnica Civil Engineering*, 65(3), 946-958.
- [31] Garmendia, L., Larrinaga, P., San-Mateos, R., & San-José, J. T. (2015). Strengthening masonry vaults with organic and inorganic composites: An experimental approach. *Materials & Design*, 85, 102-114.
- [32] Alecci, V., Focacci, F., Rovero, L., Stipo, G., & De Stefano, M. (2017). Intrados strengthening of brick masonry arches with different FRCM composites: Experimental and analytical investigations. *Composite Structures*, 176, 898-909.
- [33] Altunişik, A. C. (2011). Dynamic response of masonry minarets strengthened with fiber reinforced polymer (FRP) composites. *Natural Hazards and Earth System Sciences*, 11(7), 2011-2019.
- [34] Türkeli, E. (2020). Comparative dynamic seismic analyses of RC minarets strengthened with FRP and buttresses. *Doğal Afetler ve Çevre Dergisi*, 6(1), 119-136.
- [35] Bayraktar, A., & Hökelekli, E. (2021). A cost-effective FRCM technique for seismic strengthening of minarets. *Engineering Structures*, 229, 111672.

- [36] Tuğrulelçi, Ş. (2014). Düşey yüklenen tuğla kemerlerdeki gergi çubukların davranışa etkisinin incelenmesi (Master's thesis, Aksaray Üniversitesi Fen Bilimleri Enstitüsü).